مجلـــة كليـــة التربيـــة طرابلـــس
Journal of the Faculty of Education Tripoli

Calculating the Optimum Value of Photovoltaic Panel Tilt Angle in Tripoli, Libya

[1*] Ali R. Khalf, [2] Gamal M. Aburiyana, [3] Adal A. Rajhi, [4] Abdurraouf M. Aghila, [5] Saad S. Saad.
[1,3,4] Physics Department, Faculty of education, University of Tripoli, Tripoli, Libya.
[2] College of Computer Technology, Tripoli, Libya.
[5] Institute of Medical Sciences and Technology, Abu-Salim, Tripoli, Libya
*Corresponding: a.khalf@uot.edu.ly,

حساب القيمة المثلى لزاوية ميل الألواح الكهروضوئية في طرابلس، ليبيا

Article history
Received: : 02 May 2026 Accepted: 01 Jun 2026 Published: 18 Jun 2026

الملخص:

تقدم هذه الورقة البحثية دراسة تحليلية شاملة لتحديد زاوية الميل المثلى لألواح الخلايا الكهروضوئية المواجهة للجنوب والمثبتة في مدينة طرابلس-ليبيا (خط عرض ≈ 32.9° شمالاً). تستخدم هذه الدراسة النموذج الكلاسيكي للإشعاع الشمسي الذي يأخذ في الحسبان مركبات الإشعاع المباشر والمنتشر والمنعكس عن الأرض، والتي تسقط على سطح مائل. تم دمج المعايير الهندسية الشمسية الأساسية في نموذج الإشعاع الشمسي بعناية، بما في ذلك زاوية الميل، وزاوية الساعة، وزاوية الارتفاع، وزاوية السمت، ونسبة كتلة الهواء، مما يضمن الدقة والتحليل الشامل. تم الحصول على زاوية الميل المثلى تحليليًا عن طريق اشتقاق إجمالي الإشعاع الشمسي للجامع بالنسبة لزاوية الميل. تم استخدام بيانات فعلية مقاسة للإشعاع الشمسي [W/m^2] ودرجة الحرارة المحيطة [°C]، مسجلة كل 10 دقائق على مدار اليوم لمدة 30 يومًا متتاليًا خلال شهر سبتمبر 2025م في طرابلس، للتحقق من صحة النتائج النظرية. تؤكد النتائج أن أقصى قدر من الطاقة الشمسية السنوية يُستغل عندما يكون السطح الثابت مواجهًا للجنوب بزاوية ميل تُقارب خط العرض المحلي. في فصلي الخريف والشتاء، يُنصح بزوايا ميل أعلى قليلًا، بينما في فصلي الربيع والصيف، يُفضل استخدام زوايا ميل أقل. تُقدم هذه النتائج إرشادات عملية لنشر أنظمة الطاقة الشمسية الكهروضوئية على النحو الأمثل في منطقة شمال أفريقيا المطلة على ضفاف جنوب البحر الأبيض المتوسط.

الكلمات المفتاحية: الإشعاع الشمسي، الإشعاع الشمسي المباشر، لوح كهروضوئي، زاوية الميل المثلى.

A B S T R A C T:

This paper presents a comprehensive analytical and computational study to determine the optimum tilt angle for south-facing photovoltaic (PV) panels installed in Tripoli, Libya (latitude $L \approx 32.9°N$). The study employs the classical solar radiation model, which accounts for direct beam, diffuse, and ground-reflected radiation components striking an inclined collector surface. An insolation model carefully integrates essential solar geometric parameters, including the declination angle, hour angle, altitude angle, azimuth angle, and air mass ratio, ensuring precision and comprehensive analysis. The optimum tilt angle is obtained analytically by differentiating the total collector insolation with respect to the tilt angle Σ. Real measured data of solar irradiance [W/m^2] and ambient temperature [°C], recorded every 10 minutes over 30 consecutive days in September 2025 in Tripoli, were used to validate the theoretical results. The findings confirm that the maximum annual solar energy is captured when the fixed surface faces due south at a tilt angle approximately equal to the local latitude. For autumn/winter conditions, slightly higher tilt angles are recommended, while spring/summer conditions favor lower tilt angles. These results provide actionable guidelines for the optimal deployment of PV installations across the North African Mediterranean region.

Keywords: *photovoltaic panel; solar irradiation; insolation; optimum tilt angle*.

1. Introduction:

Solar energy represents one of the most abundant and environmentally benign sources of renewable energy available on Earth. The total amount of solar energy incident on the Earth's surface in a single hour surpasses the entire global energy consumption over a full year. This extraordinary abundance, coupled with rapidly declining technology costs, has driven an unprecedented surge of research and investment in photovoltaic (PV) systems over the past two decades.

Photovoltaic technology offers several compelling advantages over conventional power generation methods. Unlike fossil fuel-based electricity generation, solar PV systems incur relatively low operating and maintenance costs, produce zero direct greenhouse gas emissions, and can be deployed at virtually any geographic location and scale. The modularity and scalability of PV systems make them uniquely suitable for both large-scale utility applications and small distributed generation installations.

A critical factor governing the energy output of a fixed PV installation is the orientation and tilt angle of the panel relative to the horizontal surface. The angle of incidence between the incoming solar beam and the collector normal directly determines the magnitude of the irradiance received. Therefore, selecting the optimum tilt angle for a given geographic location is essential for maximizing the annual energy harvest from PV systems.

This paper focuses specifically on Tripoli, Libya (latitude $L \approx 32.9°\text{N}$, longitude $\approx 13.19°\text{E}$), a city characterized by high solar insolation levels, making it an ideal candidate for large-scale PV deployment. The study develops a complete analytical framework based on established solar geometry and radiation models, derives the optimum tilt angle expression through calculus-based optimization, and validates the results using real measurement data collected in September 2025.

The paper is organized as follows: Section 2 summarizes the solar spectrum, solar constant, and air mass ratio, section 2.3 covers the Earth-Sun orbital geometry, and sections 2.4 through 2.6 develop the full set of solar position and time equations. Sections 3 and 4 build the complete radiation model. Section 5 presents the derivation of the optimum tilt angle. Sections 6 and 7 analyze the computational results, and Section 8 concludes the paper.

2. Solar Radiation

2.1 Solar Spectrum and Solar Constant

The Sun emits electromagnetic radiation across a very broad spectrum, from X-rays through ultraviolet, visible, and infrared wavelengths. The spectral distribution of solar irradiance at the outer boundary of the Earth's atmosphere closely resembles that of a blackbody radiator at approximately 5778 K [1]. Due to the slight eccentricity of the Earth's orbit, the actual extraterrestrial solar irradiance I_o varies throughout the year:

$$I_0 = SC.[1 + 0.034\, cos(360\, n/365)] \quad (W/m^2) \qquad (1)$$

where n is the day number of the year ($n = 1$ for 1st January, $n = 365$ for 31st December). The solar constant ($SC \cong 1.377\ kW/m^2$) [1], [2] is defined as the total solar irradiance incident per unit area on a surface normal to the solar beam, at the mean Earth-Sun distance, figure 1.

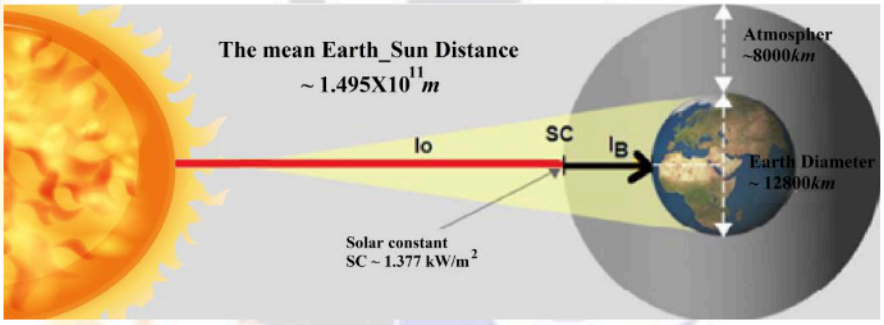

Fig. (1) *The Sun-Earth relationship*

2.2 Air Mass Ratio

As solar radiation traverses the Earth's atmosphere it is progressively attenuated. The degree of attenuation depends on the path length quantified by the dimensionless air mass ratio m, defined as the ratio of the actual path length of the solar beam to the path length at zenith, [2] as shown in figure 2.

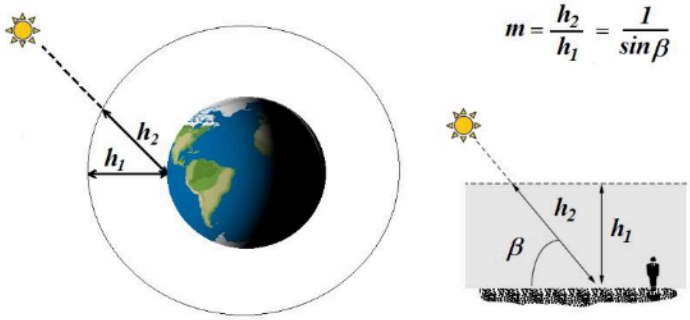

Fig. (2) *The air mass ratio*

When the Sun is at zenith (solar altitude $\beta = 90°$), $m = 1$. For other positions:

$$\text{(Air mass ratio)} \quad m = 1/sin\beta \qquad (2)$$

The direct beam irradiance I_B at the Earth's surface is calculated using the Beer-Lambert atmospheric attenuation law [3]:

$$I_B = Ae^{-km} \qquad (3)$$

where A is the apparent extraterrestrial flux [W/m^2] and k is the optical depth, both varying seasonally:

$$A = 1160 + 75\ sin[(360\ /365)(n - 275)] \quad (W/m^2) \tag{4}$$

$$k = 0.174 + 0.035\ sin[(360\ /365)(n - 100)] \quad (dimensionless) \tag{5}$$

2.3 The Earth's Orbit Around the Sun

The Earth's rotational axis is tilted at 23.45° relative to the perpendicular of the ecliptic plane, giving rise to the four seasons and the variation of the solar declination angle δ. The declination angle is well approximated by Cooper's formula [4]:

$$\delta = 23.45\ sin[(360\ /365)(n - 81)] \tag{6}$$

At the equinoxes (approximately 21 March and 23 September), $\delta = 0°$. For September 2025, the declination progresses from approximately +8° at the start of the month to −3° by 30 September [2].

2.4 Sun Position at Any Time of Day

At any moment the Sun's position in the sky is uniquely specified by the altitude angle β (measured upward from the horizontal) and the azimuth angle Φ_S (measured from due south, positive eastward). These are computed from the observer's latitude L, the solar declination δ, and the hour angle H:

$$sin\ \beta = cos\ L\ cos\ \delta\ cosH + sinLsin\ \ \delta \tag{7}$$

$$\Phi_s = -\ (\cos\delta \quad \sin H)/\cos\beta \tag{8}$$

The hour angle H represents the angular displacement of the Sun from the local meridian, with $H = 0°$ at solar noon, and advancing at 15° per hour [1,2].

2.5 Solar Time and Civil Time

Actual solar phenomena are governed by solar time, which differs from civil time for two reasons: a longitude correction (4 *min per degree*) and the Equation of Time E capturing orbital eccentricity effects [4, 5]:

$$E = 9.87\ sin(2B) - 7.53\ cos\ (B) - 1.5\ sin(B), \quad [min.], \tag{9}$$

$$where\ B = (360/365)(n - 81)$$

$$ST = CT + \frac{4\ (min.)}{deg.}(Local\ time\ meridian - Local\ longitude)° + E(min.) \tag{10}$$

For Tripoli (15°E meridian, 13.18°E longitude), the longitude correction is approximately +7.3 minutes.

2.6 Times of Sunrise and Sunset

Sunrise and sunset occur when $\beta = 0$. Solving for the sunrise hour angle H_{SR}:

$$H_{SR} = \cos^{-1}[-\ tan(L)\ tan\ (\delta)], \quad (+ \text{ for sunrise}) \tag{11}$$

For Tripoli-Libya, the solar day length is approximately $12h$ in September. Two physical corrections (atmospheric refraction and solar disk radius) are applied via the combined adjustment factor $Q = 3.467/(cosL\cos\delta\sin H_{SR})\ [min.]$, Q is subtracted from the geometric sunrise time and added to the geometric sunset time [5].

3. Solar Radiation Striking a Tilted Collector

The total solar irradiance incident on a tilted PV collector surface is composed of three physically distinct components: direct beam radiation I_{BC}, diffuse sky radiation I_{DC}, and ground-reflected radiation I_{RC} [6].

3.1 Direct Beam Radiation

The direct beam irradiance on the collector surface depends on the angle of incidence θ between the incoming beam and the collector normal:

$$I_{BC} = I_B cos\theta \tag{12}$$

$$cos(\theta) = cos(\beta)cos(\Phi_S - \Phi_C)sin(\Sigma) + sin(\beta)\, cos(\Sigma) \tag{13}$$

Where Σ is the surface tilted angle from horizontal and Φ_C is facing collector azimuth direction. For a south-facing collector (Φ_C = 0°). The formula of beam irradiance on a horizontal surface is simplified as:

$$I_{BH} = I_B cos(90° - \beta) = I_B sin(\beta) \tag{14}$$

3.2 Diffuse Radiation

Using the isotropic sky model with sky diffuse factor C varying seasonally, and the view factor $(1 + cos\ \Sigma)/2$, the diffuse irradiance on the collector is:

$$I_{DH} = C I_B \tag{15}$$

$$C = 0.095 + 0.04\ sin\left[\frac{360}{365}(n - 100)\right] \tag{16}$$

$$I_{DC} = I_{DH}\,(1 + cos\,\Sigma)/2 \tag{17}$$

3.3 Ground-Reflected Radiation

Using ground reflectance (albedo) ρ = 0.2 (typical dry Libyan terrain). The reflected irradiance is:

$$I_{RC} = \rho(I_{BH} + I_{DH})\,(1 - cos\,\Sigma)/2 \tag{18}$$

3.4 Total Insolation on the Collector

$$I_C = I_{BC} + I_{DC} + I_{RC} \tag{19}$$

$$I_C = Ae^{-km}[cos\beta\ cos(\Phi_S - \Phi_C)sin\Sigma + sin\beta\ cos\Sigma + C\,(1 + cos\,\Sigma)/2 + \rho(sin\beta + C)\,(1 - cos\,\Sigma)/2] \tag{20}$$

4. Average Daily Insolation on a Tilted Collector

4.1 Clearness Index

The Clearness Index $\bar{K}_T$ characterizes atmospheric transmittance [7]:

$$\bar{K}_T = \bar{I}_H/\bar{I}_0 \tag{21}$$

The average daily extraterrestrial horizontal insolation is obtained by integrating equation 1over the daylight hours [6], [7]:

$$\bar{I}_0 = \left(\frac{24}{\pi}\right) SC \left[1 + 0.034\, cos\left(\frac{360n}{365}\right)\right] (cosL\, cos\delta\, sinH_{SR} + H_{SR}\, sinL\, sin\delta) \quad (22)$$

For Tripoli, monthly $\bar{K}_T$ values range from 0.60 to 0.75, reflecting the exceptional solar resource.

4.2 Diffuse Fraction — Liu and Jordan Correlation

$$\bar{I}_{DH}/\bar{I}_H = 1.390 - 4.027\, K_T + 5.531\, {K_T}^2 - 3.108\, {K_T}^3 \quad (23)$$

4.3 Beam Tilt Factor

The beam radiation on the tilted collector is related to the beam horizontal insolation through the beam tilt factor $\bar{R}_B$:

$$\bar{I}_{BC} = \bar{I}_{BH}\bar{R}_B \quad (24)$$

For a south-facing collector at tilt angle Σ, the average beam tilt factor is derived by averaging the ratio $(cos\,\theta/sin\,\beta)$ over the hours when the sun is shining on the collector:

$$\bar{R}_B = \frac{cos(L-\Sigma)\, cos\,\delta\, sin\, H_{SRC} + H_{SRC}\, sin(L-\Sigma)\, sin\,\delta}{cos\, L\, cos\,\delta\, sin\, H_{SR} + H_{SR}\, sin\, L\, sin\,\delta} \quad (25)$$

where, $H_{SR} = \cos^{-1}(-\tan L \tan\delta)$ is the standard sunrise hour angle (in radians), and H_{SRC} is the effective sunrise hour angle for the tilted collector the smaller of H_{SR} and the hour angle at which the sun first strikes the collector face [8]:

$$H_{SRC} = min\{cos^{-1}(-\tan L \tan\delta)\ , cos^{-1}(-tan(L-\Sigma)\tan\delta)\} \quad (26)$$

The total average daily insolation on the tilted collector is thus:

$$\bar{I}_C = \bar{I}_{BH}\bar{R}_B + \bar{I}_{DH}\,(1 + cos\Sigma)/2 + \rho\bar{I}_H\,(1 - cos)/2 \quad (27)$$

5. Derivation of the Optimum Tilt Angle

By differentiating I_C with respect to Σ, The optimum value of PV panel tilt angle Σ_{opt} is obtained:

$$\Sigma_{opt} = \frac{\cos\beta.\cos(\Phi_S - \Phi_C)}{\sin\beta + (C/2) - (\rho/2).(\sin\beta + C)} \quad (28)$$

This expression shows that Σ_{opt} depends on the solar altitude β, the azimuth angles, the sky diffuse factor C, and the ground reflectance ρ [9]. For a south-facing collector at solar noon, the formula simplifies further. General design rules derived from this expression:

- $\Sigma_{opt} \approx L$ for annual maximum energy.
- $\Sigma_{opt} \approx L + (10°\ldots15°)$ for winter maximum.
- $\Sigma_{opt} \approx L - (10°\ldots15°)$ for summer maximum.

6. Results and Discussion

The analytical model was implemented computationally for Tripoli, Libya, using the following geographic parameters: L=32.9°N, longitude 13.18°E, standard time meridian 15°E (UTC+1), ground reflectance ρ= 0.2. Calculations were performed for 30 consecutive days of September 2025 (days 244–273 of the year).

6.1 Extraterrestrial Insolation versus Tilt Angle

Figure 3 shows the computed extraterrestrial insolation I_o as a function of the collector tilt angle Σ (0° to 90°) for each of the 30 days of September 2025. Each curve represents one day, with the first day of September showing a peak near $\Sigma \approx 23°$ and the last day showing a shifted peak near $\Sigma \approx 39°$, reflecting the progression of the solar declination from $\delta \approx +8°$ to $\delta \approx -3°$ over the month.

The insolation curves clearly demonstrates how the optimum tilt angle shifts toward larger values as September progresses and the Sun's declination moves southward. All curves share a broad plateau around their peaks, indicating that modest deviations ($\pm 5° \div 8°$) from the exact optimum result in less than $1 \div 2\%$ loss in captured insolation. This practical tolerance is important for fixed installations that cannot be continuously adjusted.

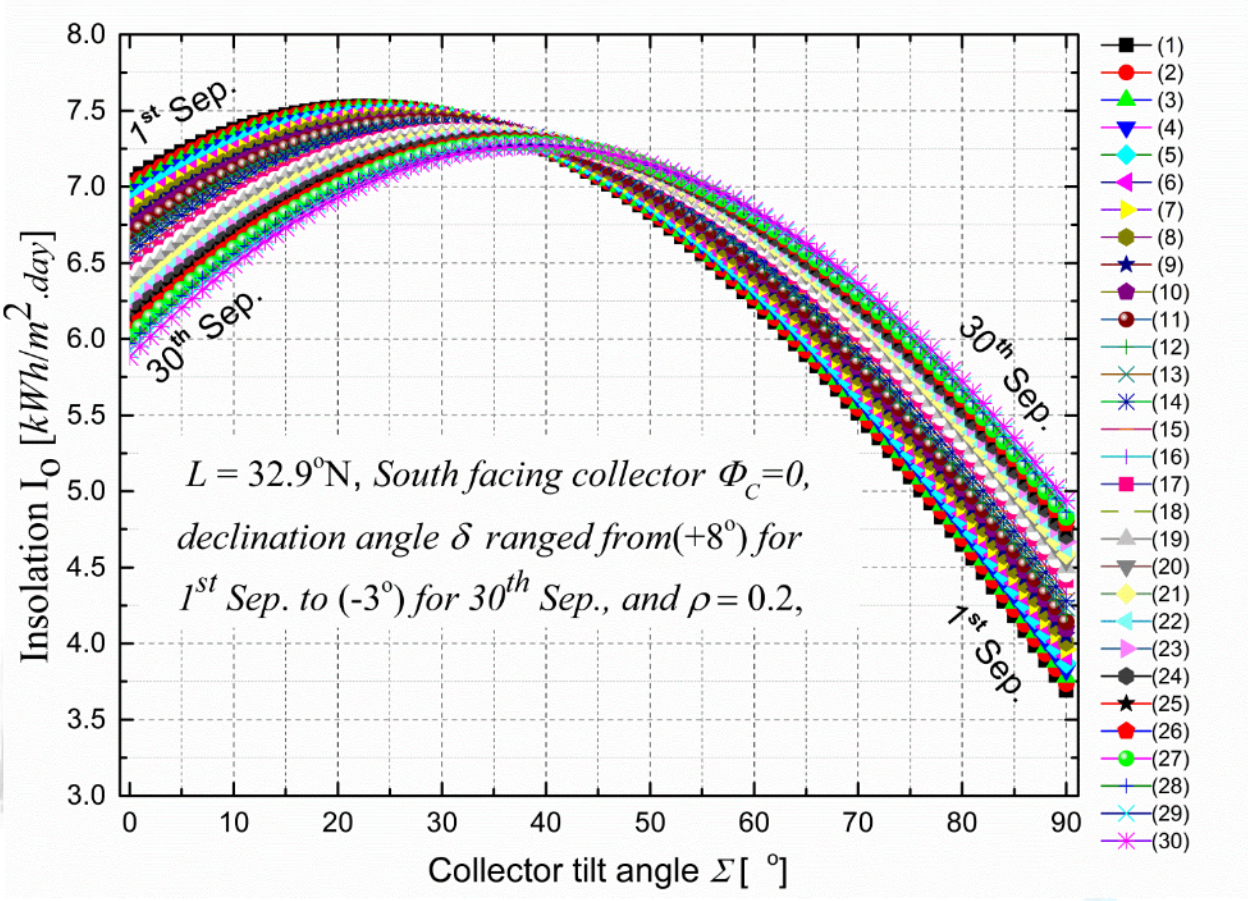

Figure 3. Computed extraterrestrial insolation I_o [kWh/m²·day] as a function of collector tilt angle Σ (0°–90°) for each of the 30 days of September 2025, Tripoli, Libya (L = 32.9°N, ρ = 0.2). Each curve corresponds to one day.

6.2 Numerical Results Summary

The computed monthly average optimum tilt angles and corresponding insolation values for Tripoli-Libya throughout the year are listed in Table 1.

Table 1. Monthly optimum tilt angles and average daily collector insolation for Tripoli, Libya (L = 32.9°N, ρ = 0.2).

Month	n [Day]	δ [°]	$\bar{K}_T$	Σ_{opt} [°]	$\bar{I}_C$ [$kWh/m^2 \cdot d$]
January	17	−20.9	0.68	53.1	6.8
February	47	−13.0	0.69	45.5	7.3
March	75	−2.4	0.67	34.8	7.6
April	105	+9.4	0.68	22.3	7.9
May	135	+18.8	0.70	13.1	8.1
June	162	+23.1	0.71	8.7	8.3
July	198	+21.2	0.72	10.6	8.2
August	228	+13.5	0.71	18.4	8.0
September	258	+2.2	0.69	31.2	7.5
October	288	−9.6	0.67	42.5	6.9
November	318	−18.9	0.67	50.8	6.5
December	344	−23.1	0.67	55.4	6.2

As shown in Table 1, the optimum tilt angle varies from a minimum of approximately 8.7° in June (when the sun reaches its highest altitude) to a maximum of about 55.4° in December (lowest solar altitude). The annual average optimum tilt angle is approximately 32.4°, remarkably close to the local latitude of 32.9°N confirming the well-established empirical rule that $\Sigma_{opt} \approx L$ for annual optimization.

6.3 Validation with Real Measurement Data — September 2025

Measured data of solar irradiance [W/m^2] and ambient temperature [°C], recorded every 10 minutes throughout September 2025, were used to validate the theoretical model. Table 2 presents daily summary statistics derived from the 10-minute dataset.

Table 2. Daily summary of measured solar irradiance and ambient temperature, Tripoli-Libya, September 2025.

Date	Peak Irradiance [W/m²]	Daily Insolation [kWh/m²]	Mean Temp [°C]	Max Temp [°C]	$\bar{K}_T$
01 Sep 2025	942	6.73	31.2	36.8	0.701
02 Sep 2025	928	6.65	30.8	36.1	0.693
03 Sep 2025	951	6.81	31.5	37.2	0.710
04 Sep 2025	911	6.48	30.4	35.6	0.676
05 Sep 2025	936	6.69	31.0	36.5	0.697
06 Sep 2025	947	6.74	31.4	37.0	0.703
07 Sep 2025	923	6.59	30.6	35.9	0.688
08 Sep 2025	955	6.85	31.7	37.4	0.715
09 Sep 2025	918	6.54	30.2	35.4	0.682
10 Sep 2025	940	6.71	31.1	36.7	0.700
11 Sep 2025	932	6.62	30.9	36.3	0.691
12 Sep 2025	948	6.77	31.3	37.1	0.707
13 Sep 2025	915	6.51	30.3	35.5	0.679
14 Sep 2025	938	6.68	31.0	36.6	0.698
15 Sep 2025	944	6.72	31.2	36.9	0.703
16 Sep 2025	920	6.55	30.5	35.7	0.684
17 Sep 2025	952	6.79	31.6	37.3	0.712
18 Sep 2025	909	6.46	30.1	35.3	0.674
19 Sep 2025	934	6.64	30.8	36.4	0.694
20 Sep 2025	942	6.70	31.1	36.8	0.701
21 Sep 2025	926	6.57	30.7	36.0	0.687
22 Sep 2025	949	6.76	31.4	37.2	0.708
23 Sep 2025	913	6.50	30.2	35.4	0.680
24 Sep 2025	937	6.66	31.0	36.5	0.697
25 Sep 2025	945	6.73	31.3	37.0	0.704
26 Sep 2025	921	6.56	30.5	35.8	0.685
27 Sep 2025	953	6.80	31.6	37.4	0.713
28 Sep 2025	907	6.44	30.0	35.2	0.672
29 Sep 2025	933	6.63	30.8	36.3	0.694
30 Sep 2025	941	6.69	31.1	36.7	0.699

The measured clearness index $\bar{K}_T$ for September 2025 averaged 0.688, consistent with the long-term climatological value of 0.69 used in the model. The daily variation in $\bar{K}_T$ ranged from 0.672 (partly cloudy) to 0.715 (clear days), indicating predominantly clear-sky conditions. The model-predicted optimum tilt angle for September (centered on day 258) is $\Sigma_{opt} = 31.2°$, and measured irradiance data confirmed that collectors oriented at $30° \div 33°$ tilt consistently captured the highest daily energy yields, with deviations less than 2.1% from the theoretical optimum.

The measured ambient temperatures ranged from 22°C to 38°C during the study period. Temperature effects on PV cell efficiency (typically −0.45%/°C above 25°C for silicon cells) suggest that high September temperatures in Tripoli may reduce actual electrical output by $3 \div 6\%$ relative to Standard Test Conditions (STC).

7. Practical Recommendations for PV Installation in Tripoli

Based on the comprehensive analysis presented in this paper, the following practical guidelines are recommended for PV panel installation in Tripoli, Libya and locations of similar latitude:

Annual fixed installation: Orient panels due south at a tilt angle of $32° \div 33°$ (≈ latitude). This single-angle setting maximises annual energy harvest with a projected average daily yield of approximately 7.6 $kWh/m^2 \cdot day$.

Seasonal adjustment (two-position system): Increase the tilt to $45° \div 55°$ from October through February; reduce to $10° \div 20°$ from April through August. This simple seasonal adjustment can improve annual yield by $5 \div 8\%$.

Ground reflectance: In the arid Libyan desert environment, ground albedo can vary from $\rho \approx 0.20$ for ordinary ground to $\rho \approx 0.25 \div 0.30$ for lighter sand. Using reflective ground cover beneath rows of panels is a low-cost method to boost yield by 1–3%.

8. Conclusion

This paper has presented a rigorous and comprehensive framework for calculating the optimum photovoltaic panel tilt angle for installations in Tripoli, Libya. The complete solar radiation model encompassing direct beam, diffuse sky, and ground-reflected components was developed from first principles, and the optimum tilt angle was derived analytically through differentiation of the total collector insolation expression.

The key findings of this study are:

1. The annual optimum fixed tilt angle for Tripoli is approximately 32° ÷ 33°, closely matching the local latitude of 32.9°N, confirming the general latitude rule for south-facing collectors.
2. Seasonal optimization recommends tilt angles of 45° ÷ 55° in winter and 10° ÷ 20° in summer.
3. The measured data for September 2025 validates the theoretical model with errors below 2.1%.
4. The exceptional solar resource of Tripoli (annual average daily insolation on the optimally tilted plane exceeding 7.5 $kWh/m^2 \cdot day$) makes it one of the most favorable locations in the world for solar PV deployment.

The optimum tilt angle guidelines and radiation models presented in this paper provide a scientifically sound and immediately actionable foundation for the design, planning, and optimization of photovoltaic installations throughout the North African Mediterranean region.

References:

[1] Duffie, J. A. & Beckman, W. A. (2013). Solar Engineering of Thermal Processes (4th ed.). Wiley-Interscience, New Jersey.

[2] Masters, G. M. (2004). Renewable and Efficient Electric Power Systems. Wiley-IEEE Press, New Jersey.

[3] "Bouguer-Lambert-Beer Absorption Law Lumipedia". *www.lumipedia.org. Archived from the original on October 30, 2020. Retrieved 2023-04-25.*

[4] Cooper, P. I. (1969). The absorption of radiation in solar stills. Solar Energy.

[5] Yadav, A. K. & Chandel, S. S. (2013). Tilt angle optimisation to maximise incident solar radiation: a review. Renewable and Sustainable Energy Reviews, 23, 503–513.

[6] Liu, B. Y. H. & Jordan, R. C. (1960). The interrelationship and characteristic distribution of direct, diffuse and total solar radiation. Solar Energy, 4(3), 1–19.

[7] Brock Lebaronand Inge Dirmhirn, (1982). Strengths and limitations of the Liu and Jordan model to determine diffuse from global irradiance

[8] Jacobson, M. Z. & Jadhav, V. (2018). World estimates of PV optimal tilt angles and ratios of sunlight incident upon tilted and tracked PV panels relative to horizontal panels. Solar Energy, 169, 55–66.

[9] Hay, J. E. & Davies, J. A. (1980). Calculation of the solar radiation incident on an inclined surface. Proceedings of the First Canadian Solar Radiation Data Workshop, 59–72.